REPORT DOCUMENTATION PAGE

Form Approved
OMB No. 0704-0188

1. AGENCY USE ONLY (Leave blank)	2. REPORT DATE	3. REPORT TYPE AND DATES COVERED
	3/8/94	Technical Report /June '93-May '94

4. TITLE AND SUBTITLE
DIMERIZED PI-COMPLEXES IN SELF_ASSEMBLED MONOLAYERS CONTAINING VIOLOGENS: AN ORIGIN OF UNUSUAL WAVESHAPES IN THE VOLTAMMETRY OF MONOLAYERS

5. FUNDING NUMBERS
Grant # N00014-90-J-1167
R&T Code 4133019

6. AUTHOR(S)
Xiaoyan Tang and Daniel A. Buttry

7. PERFORMING ORGANIZATION NAME(S) AND ADDRESS(ES)
Department of Chemistry, University of Wyoming
Laramie, WY 82071-3838

8. PERFORMING ORGANIZATION REPORT NUMBER

9. SPONSORING/MONITORING AGENCY NAME(S) AND ADDRESS(ES)
Office of Naval Research
Chemistry Division
800 N. Quincy Street
Arlington, VA

10. SPONSORING/MONITORING AGENCY REPORT NUMBER
Technical Report
24

11. SUPPLEMENTARY NOTES
Prepared for publication in Langmuir

12a. DISTRIBUTION/AVAILABILITY STATEMENT
This document has been approved for public release and sale; its distribution is unlimited

12b. DISTRIBUTION CODE

13. ABSTRACT *(Maximum 200 words)*

Abstract-Thiol derivatives of viologens self-assemble at gold and silver electrodes to give monolayers with relatively high surface coverages. Lateral interaction of the viologen redox groups in these monolayers is revealed by virtue of the formation of unique π-complex dimers (pi-mers) for the one-electron reduced form of viologens within these monolayers. The presence of these pi-mers is shown to give double-peaked voltammetric waves, and is unambiguously observed in the surface Raman (including SRRS, SERS and SERRS) spectra of these monolayers. The Raman bands due exclusively to the pi-mer as previously reported are assigned to the out-of-phase coupling modes of the totally symmetric ring modes of the component cation radicals in the pi-mer.

14. SUBJECT TERMS	15. NUMBER OF PAGES
electrochemistry, self-assembly, monolayer	42
	16. PRICE CODE

17. SECURITY CLASSIFICATION OF REPORT	18. SECURITY CLASSIFICATION OF THIS PAGE	19. SECURITY CLASSIFICATION OF ABSTRACT	20. LIMITATION OF ABSTRACT
unclassified	unclassified	unclassified	UL

OFFICE OF NAVAL RESEARCH

Grant # N00014-90-J-1167

R&T Code 4133019

Technical Report #24

Dimerized π-Complexes in Self-Assembled Monolayers Containing Viologens: An Origin of Unusual Waveshapes in the Voltammetry of Monolayers

by

Xiaoyan Tang and Daniel A. Buttry

Prepared for Publication in

Langmuir

Department of Chemistry
University of Wyoming
Laramie, WY 82071-3838

March 3, 1994

DIMERIZED π-COMPLEXES IN SELF-ASSEMBLED MONOLAYERS CONTAINING VIOLOGENS: AN ORIGIN OF UNUSUAL WAVESHAPES IN THE VOLTAMMETRY OF MONOLAYERS

Xiaoyan Tang and Daniel A. Buttry

Department of Chemistry

University of Wyoming

Laramie, WY 82071-3838

Abstract-Thiol derivatives of viologens self-assemble at gold and silver electrodes to give monolayers with relatively high surface coverages. Lateral interaction of the viologen redox groups in these monolayers is revealed by virtue of the formation of unique π-complex dimers (pi-mers) for the one-electron reduced form of viologens within these monolayers. The presence of these pi-mers is shown to give double-peaked voltammetric waves, and is unambiguously observed in the surface Raman (including SRRS, SERS and SERRS) spectra of these monolayers. The Raman bands due exclusively to the pi-mer as previously reported are assigned to the out-of-phase coupling modes of the totally symmetric ring modes of the component cation radicals in the pi-mer.

Introduction

The preceding paper (1) describes a direct comparison of the spontaneous adsorption of viologen derivatives bearing thiol and disulfide pendent groups to form self-assembled monolayers (SAM's) on Au electrodes. A prominent feature in the voltammetry of the SAM's formed from the thiol derivatives is the presence of a very well-defined, double-peaked voltammetric wave at the redox potential for the first reduction of the viologen redox group to the one-electron reduced cation radical species. The sharper and more positive of these two peaks was attributed to the formation of a unique π-stacked dimer of adjacent cation radicals within the monolayer. In this second paper, we present vibrational spectroscopic evidence for the formation of these π-complexes, and show that the appearance of the spectroscopic signatures of the π-comlex dimer are coincident with the appearance of this sharp peak in the voltammetry.

Cyclic voltammetry is a frequently used electrochemical method for studying electroactive monolayers formed by either self-assembly or the Langmuir-Blodgett method. The theory of the voltammetric response of a monolayer of an immobilized redox species predicts, if the surface redox-electrode reaction is reversible, that the peak current i_p is proportional to the potential scan rate v, that the peak potentials and waveshapes for the cathodic and anodic surface waves are identical, and that the full width at half maximum of the wave, E_{FWHM}, equals 90.6/n mV

where n is the number of electrons transferred in the redox reaction (2). These theoretical predictions are frequently not followed in experimental results. In particular, unusual double peaked voltammetric waves have been observed in several cases, including those in which the redox reaction is thought to involve only one electron per redox group. For instance, both Bard's and our groups have reported double voltammetric peaks for the first reduction wave of monolayers of viologen derivatives (3-6). This unusual double peak phenomenon has also been observed for monolayers of other molecules (7). The origin has not been clear in these previous studies. However, most of these previous studies show that this unusual waveshape is related to the closeness of the redox moieties in the monolayer. Various models have been developed to predict such non-ideal voltammetric responses. These models produce different non-ideal waveshapes by adjusting a variety of empirical fitting parameters. For example, according to the theoretical model developed by Tokuda et al. (8,9), the double voltammetric peaks result when two parameters (out of a total of six), the interaction parameter and coordination number, reach certain values. While these model fitting parameters can characterize the departure of experimental cyclic voltammograms from ideal behavior, they are not related to the specific molecular properties of the monolayer in a straightforward manner. In other words, they do not elucidate the <u>microscopic</u> molecular behavior that leads to these unique voltammetric responses. It is precisely this type of correlation between the macroscopic voltammetric

results and the microscopic molecular environment that we seek in the present study. Toward this end, we have employed spontaneous adsorption of sulfur bearing redox molecules (4,5) to create self-assembled monolayers that can be used to address this issue.

Thiol derivatives of viologens have been shown to self-assemble at gold electrodes to give monolayers of high coverage (1,4,5). Accompanying this high coverage is the appearance of double voltammetric peaks for the first reduction wave. In this contribution, the reduction to cation radicals (the one-electron reduced form) of the viologen redox moiety in these monolayers on gold and silver electrodes is probed using surface Raman spectroscopy under conditions of surface enhancement and/or resonance enhancement. Formation of dimerized π-complexes in the one-electron reduced form of viologens in these monolayers is unambiguously observed in the surface Raman spectra of these monolayers, and the appearance of the double voltammetric peaks is attributed to the formation of the pi-mer in the monolayer.

Experimental

The silver or gold electrode was constructed from flattened high purity silver or gold wire that was sealed in a Teflon plug with Torr Seal. The electrode surface (either silver or gold) was polished mechanically using increasingly smaller sizes of alumina powder (to 0.05 μm) and washed ultrasonically in deionized water. The roughened silver electrode was prepared by a double potential step sequence of -0.2 to +0.2 V and back to -0.2 V versus SSCE in

0.1 M NaCl, with a dwell time of 3 to 4 s at +0.2 V, using a PAR Model 273 potentiostat. The dimensions of the exposed, rectangular electrode were ca. 1 x 10 mm. The Raman cell that was used to obtain surface Raman spectra was constructed in the shape of a cylinder with an optically flat window. A Ag/AgCl electrode served as a reference electrode and a platinum wire was used as the counter electrode. After assembly of the SAM, the silver or gold electrode was used as the working electrode. The electrolyte in the Raman cell was deaerated by purging with argon before the experiment. Careful attention to exclusion of air is required for these experiments due to the extreme sensitivity of the reduced forms of viologens to oxygen.

The compounds are referred to in the following way: $CH_3V^{2+}(CH_2)_{12}SH$, where V^{2+} designates the viologen redox group, is referred to as 1V12SH, with the numbers referring to the number of carbons in the alkyl chain. Other compounds are referred to analogously. 1V12SH and 1V16SH were synthesized by the method described in reference 1. Synthesis of compounds 1V3V1 (a dimeric viologen with a propyl spacer group between the ring systems) and 2V12 (a long chain viologen derivative capable of micellization) was accomplished by the method in references 10 and 11, respectively. All other chemicals were used as received. Monolayers of all thiol derivatives were formed by immersing the polished or roughened electrode into a dilute aqueous electrolyte solution of the compound of interest for a time period ranging from a few hours to days. Following assembly, rinsing in pure

electrolyte may be needed for a few times to remove non-chemisorbed materials.

In-situ Raman spectra were obtained using a Raman system that has been described previously (12). The uv-vis absorption spectra were taken on a Perkin Elmer Lambda 9 UV/VIS spectrometer.

Results and Discussion

Electronic spectra

As is well known, viologen dications are reduced to cation radicals in the first reduction process. The cation radicals have been assumed to have a co-planar conformation of the two pyridyl rings (13) and are known to dimerize in some solutions including aqueous solutions. The dimerization has been studied by uv-vis absorption spectroscopy and electron spin resonance spectroscopy.

Schwarz (14) studied the uv-vis absorption of solutions of methylviologen cation radical $MV^{+\cdot}$ produced electrochemically over the concentration range in which an obvious color change occurs. He confirmed that a monomer-dimer equilibrium is involved, with K_{diss} = 2.6 x 10^{-3} M at room temperature as shown by the equation below. The difference between the absorption spectrum of the dimer and

$$(MV^{+\cdot})_2 \overset{K_{diss}}{\rightleftharpoons} 2MV^{+\cdot}$$

that of the monomer includes a new band at longer wavelength (ca. 870 nm) and a blue shift both in the visible and near uv absorption

bands with some loss of fine structure. A diradical dimer structure was assumed by Kosower and co-workers based on the absorption spectra (15). The ESR results by Evans and co-workers (16,17) showed that the paramagnetic cation radical is in equilibrium with a diamagnetic dimeric species and that, as indicated by their ΔS^0 data, dimerization involves extensive desolvation. This suggested that in the dimer the two cation radicals are arranged in a face-to-face configuration. The requirement for a face-to-face configuration has been elegantly demonstrated for intramolecular association of two pendent pyridinyl radicals (18-20) and two pendent viologen cation radicals (21-25) in systems in which the two chromophores were linked by an n-CH_2 chain with n being an integer larger than 1. Two forms of the diradicals were postulated (18): closed and open. The trimethylene (when n=3) chain which is most efficient for reaching a face-to-face configuration of the two chromophores in the closed form was proved to be most efficient for intramolecular dimeric association. Thus, when n=3 a strong intramolecular association (ca. 90%) occurred even at room temperature. To the contrary, when n=2 the intramolecular association was structurally inhibited. In a related study, Cotton and coworkers showed that cation radicals of the asymmetric viologens containing alkyl substituents with chain lengths exceeding C_8 (such as $1V12^{+\cdot}$) will dimerize to a large extent (>80%) (26). This was attributed to the tendency for these longer chain viologens to associate into micelles, which increases the local concentration of cation radicals at the surface of the

micelle and increases dimerization.

It is clear that the reversible dimerization of these species is not through σ-covalent bond formation but through π-π interaction which is achieved by π^*-orbital overlap between the singly occupied π^*-orbitals of the two cation radicals. This requires a face-to-face geometry of the two π-systems and a specific orientation determined by the symmetries of the two overlapping π^*-orbitals. This kind of dimerization was first reported by Hausser in 1957 (27). Kosower has given the name pi-mer to the dimer formed by this kind of interaction, with the corresponding dimerization being called pi-merization (28,29). The new absorption band due to pi-mer formation at wavelengths longer than the absorption bands of the monomer (e.g. at ca. 900 nm in Figure 1) has been assigned as a charge-transfer band between the two components in the pi-mer, and the Mulliken charge transfer theory was used to interpret the spectral properties of these complexes (27).

These previous results are corroborated by the data in Figure 1, which shows the uv-vis spectra of separate aqueous solutions of MV^+, $1V12^+$, and $1V^+3V^+1$, prepared by stoichiometric, one electron reduction of the appropriate viologen precursor using dithionite. In curve C, the MV^+ is present below the concentration necessary to produce the pi-mer, so its spectrum is characteristic of the monomeric form of the paramagnetic cation radical of the viologen redox group. The $1V^+12$ solution is prepared under conditions at which the cationic, long chain viologen radical cations will form

micelles. As prevously indicated by Cotton et al. (26), this leads to pi-merization, as shown by the presence of the absorption band at ca. 900 nm and the blue shift of the band centered near 600 nm, relative to that in MV^+. Finally, the solution of $1V^+3V^+1$ also shows the long wavelength band and blue shift of the higher energy visible band previously attributed to pi-merization of this species (21-25). Inspection of these three spectra reveals that the MV^+ solution contains only monomer, the $1V^+3V^+1$ solution contains only pi-mer, and the $1V^+12$ solution contains some of each. The figure also shows the positions of the laser lines at 457, 488, and 514.5 nm that were used in the Raman characterization of these solutions, as well as the viologen SAM's, to be described below. These spectra clearly show that it is possible to produce high concentrations of these unique pi-mers, given appropriate conditions.

Vibrational spectra of monomer and pi-mer

There have been several previous studies of the Raman spectrum of MV^+. In the wavenumber region of 1000-1700 cm^{-1}, the resonance Raman spectrum of a dilute solution of $MV^{+\cdot}$ shows four strong bands at 1028, 1356, 1534 and 1662 cm^{-1}, respectively. These were all assigned to fundamental, totally symmetric ring modes of the monomeric species (26,30-32). In more concentrated solutions where the pi-mer concentration can be calculated from the value of K_{diss} reported by Schwartz (14), Hester and coworkers reported the presence of some completely new bands, as well as several bands whose intensity increased as a function of concentration by a greater factor than the concentration increase (30). These bands

were attributed to a dimeric species (i.e. the pi-mer). Basically, the pi-mer bands are shifted by ca. -20 cm^{-1} on average as compared with the monomer, assuming the wavenumber correlations 1028/1028, 1356/1340, 1534/1512, -/1534, 1662/1604 for $MV^{+\cdot}/(MV^{+\cdot})_2$. Note that Hester and coworkers assigned the 1534 cm^{-1} band to the pi-mer but could not find its counterpart in the monomer. More importantly, their depolarization ratios of the pi-mer bands at 1340 and 1512 cm^{-1}, respectively, measured in a saturated aqueous $MV^{+\cdot}$ solution, showed that these bands are fully depolarized and may even show slightly inverse polarization ($\rho \sim 0.9$). This shows that these pi-mer bands cannot be fundamental A_g ring modes while the corresponding monomer bands are, a point to which we will return below.

Evidence for the cation radical pi-mer formation has also been provided by infrared spectroscopy (33-36). The occurrence of the dimeric association was proved by observing the fundamental, totally symmetric ring modes (which should be forbidden in the IR) with abnormally strong intensities in the infrared spectra of the cation radical. The strong intensity enhancement of these forbidden A_g ring modes has been attributed to electron-molecular vibration (e-mv) interactions, which were first reported for the donor-acceptor charge transfer complex between benzene and iodine and discussed in the context of the CT theory (37) by Ferguson and Matsen (38) in 1958. The idea behind this model is that both the ionization potential and electron affinity are generally expected to depend on the instantaneous nuclear geometry of a molecule, and

therefore, are functions of the normal modes of vibration. As a result, in a CT complex, motion during a particular intramolecular vibration of either donor or acceptor may cause redistribution of electrons. Thus, the vibration within the CT complex will be strongly coupled to the charge transfer transition, leading to the e-mv coupling originally described by Ferguson and Matsen (38). This kind of e-mv interaction in CT complexes has been very well studied in a variety of quasi-one-dimensional organic charge transfer crystals by Pecile and co-workers (39) and Rice and co-workers (40).

According to the model proposed by Rice and coworkers (40), another consequence of the e-mv coupling is that the vibrational frequency w_i is lowered in the complex with respect to that (w_i°) of the unperturbed mode in the free molecule by an amount that is a function of the extent of mixing of the radical molecular orbitals in the CT complex and the magnitude of the redistribution of electron density during the vibration in the complex. This frequency lowering due to e-mv coupling was observed in both the infrared and Raman spectra of the CT crystals studied. In the case of a radical-radical, self-dimeric CT complex (of which $(MV^+)_2$ is an example), it was shown that any two degenerate, totally symmetric normal modes (Q_{i1} and Q_{i2}) of the two component molecules can couple to give in-phase (s_i) and out-of-phase (q_i) vibrational modes and that the in-phase modes are completely decoupled from the CT transition, whereas the out-of-phase modes q_i are coupled to the CT transition. Conceptually, this can be described as electron

oscillation back and forth from one component radical to the other induced by the out-of-phase q_i modes. The in-phase modes s_i are only Raman active and their frequencies are not disturbed and are, therefore, identical with those of Q_i. Due to the coupling to the CT transition, the out-of-phase q_i modes are both infrared and Raman active and their frequencies are lowered with respect to those of Q_i. In addition, for the out-of-phase q_i modes, the electron oscillation, and therefore the dipole moment and polarizability changes, are predominantly perpendicular to the molecular plane. This polarization of the infrared bands has been confirmed by experiments on oriented CT complexes (37,41-43). Finally, we note that the frequencies of the strong infrared absorption bands for viologen radical cations that have been attributed to vibronic activation of the A_g ring modes (33-36) are coincident with those of the lower energy bands attributed to the pi-mer in the resonance Raman spectra (30).

Based on all the previous results and the above discussion, we assign the lower energy bands that were attributed to the pi-mer by Hester and co-workers (30) to the out-of-phase coupling modes q_i of the A_g ring modes Q_i. Thus $(MV^+)_2$ has two Raman bands: q_i and s_i while MV^+ shows only Q_i, as shown in Table 1. This assignment has at least one consequence that is related to the fact that, while Q_i and s_i are totally symmetric modes, q_i is not. Thus, since the resonance Raman intensity enhancements of totally symmetric modes are typically much larger than those of modes with lower symmetry (44), one expects that excitation in resonance with a pi-mer

electronic absorption band would lead to preferential enhancement of s_i compared to q_i, while excitation off-resonance would eliminate this preferential enhancement. Of course, a more trivial consequence of excitation in resonance with a pi-mer electronic absorption would be preferential enhancement of pi-mer Raman bands compared to monomer Raman bands. In addition, this assignment is consistent with the seemingly anomalous depolarization ratios reported by Hester and coworkers (30), and discussed above. As will become clear below, this assignment is important to the present study of pi-merization in viologen SAM's for two reasons. First, it allows us to unambiguously demonstrate the presence of pi-mers within the SAM using Raman spectroscopy. Second, this assignment defines the predominant direction of the transition moment for the CT transition in the pi-mers and the polarizability change for the q_i modes that are vibronically coupled to it as perpendicular to the molecular planes of the two ring systems in the pi-mer. This second point can thus be used in arguments as to the relative orientation of the pi-mer ring systems with respect to the electrode surface.

Given this new assignment of the pi-mer vibrational bands, we turn to an examination of their excitation profiles and concentration dependence. Figure 2 shows the Raman spectra of a 5 mM solution of $MV^{+\cdot}$ at two different excitation wavelengths. These spectra show the pi-mer q_i bands at 1340 and 1512 cm^{-1}, and the pi-mer s_i bands at 1356 and 1534 cm^{-1}, respectively. Referring to Figure 1, it can be seen that 514 nm excitation is on-resonance

with a pi-mer electronic transition, while 457 nm excitation is not. Focusing on the q_i and s_i bands at 1512 and 1534 cm^{-1}, respectively, one can clearly see that the ratio of intensities of s_i to q_i is much larger at 514 nm (on-resonance) than at 457 nm (off-resonance), in complete agreement with expectations. Another interesting feature of these data is that the 1534 cm^{-1} band is considerably more enhanced than the 1356 cm^{-1} band with 514 nm excitation. This is likely an indication that the 1534 cm^{-1} band is more strongly vibronically coupled to the 536 nm pi-mer electronic transition than is the 1356 cm^{-1} band (46). However, the assignment (32) of these two bands as being predominantly derived from a ring breathing mode (1534 cm^{-1}) and the inter-ring C-C stretch (1356 cm^{-1}) does not make it obvious why this should be the case. In fact, one could argue that this situation should be reversed, since the frequency of the 1534 cm^{-1} ring mode is only weakly dependent on the oxidation state of the viologen (and, therefore, the electron density in the π^* system), while that of the 1356 cm^{-1} inter-ring C-C stretch is quite strongly dependent on oxidation state (32).

Another consequence of the above assignment is that since [D]/[M] increases as C_{total} increases, the intensities of the q_i modes should increase compared to the intensities of the s_i and Q_i modes (I_{Qi+si}) as C_{total} increases. This is exactly what Figure 3 shows. The increase in I_{1512} compared to I_{1534} in Figure 3B is not as large as that in Figure 3A because, when using 514 nm excitation, the monomer Q_i modes do not contribute to I_{Qi+si} as much

as in the case of Figure 3A which used 457 nm excitation. Note also that at a total concentration (C_{total}) of ca. 7 mM the monomer and pi-mer concentrations are approximately equal (from K_{diss}), so the data in Figure 3 allow one to make a crude assessment of the relative Raman cross-section of the monomer and pi-mer at these excitation wavelengths.

Figure 4 shows another example of a viologen system in which pi-merization is important. These Raman spectra, at several excitation wavelengths, are for the one-electron reduced form of $1V12^{+\cdot}$ at a total concentration of ca. 0.3 mM. It has been previously shown (26) that these cation radicals form micellar aggregates under these conditions. These spectra clearly show the predominance of the low energy q_i band for these solutions, indicative of a significant level of pi-merization in this system, presumably due to the high local concentration of radical cations at the surface of the micelle. Also, once again one can see the enhanced intensity of the pi-mer s_i band (at 1534 cm^{-1}) compared to the pi-mer q_i band (at 1512 cm^{-1}) with 514 nm excitation compared to 457 nm excitation.

Figure 5 shows the Raman spectra of a ca. 1 mM solution of $1V^{+}3V^{+}1$ (produced from the parent viologen dimer, $1V^{2+}3V^{2+}1$ by stoichiometric reduction with one electron per viologen) at several excitation wavelengths. As discussed above, and shown in Figure 1, this system pi-merizes essentially completely under these conditions. However, the Raman spectrum shows no evidence for the low energy bands (i.e. the q_i bands) that would normally be

attributed to the pi-mer. Instead, only a single set of bands is observed, and these are at the frequencies of the monomer Q_i and/or pi-mer s_i bands (e.g. at 1534 and 1356 cm^{-1}). The origin of this behavior is not clear. However, it is possible to speculate on it based on the CT models that have been previously applied to these systems (39,40). These models arise from treatments based on a weak coupling between the two radicals in the dimer. In the formalism of the Mulliken charge transfer theory, this statement is equivalent to saying that the coefficient of the CT dative state, b, which gives a fractional representation of the mixing of the electron density of the two radicals in the dimer, is not too large. However, in the $1V^{+}3V^{+}1$ case, the very close approach of the two radical ring systems forced by the n=3 linkage leads to extremely good overlap of the two MO's and consequently strong mixing of the two radical MO's in this pi-mer. In this case, b will be large (approximately 1), and the electron-molecular vibration model derived by Rice (40) will not be applicable. Under these conditions, it is probably inappropriate to think of charge oscillation between rings driven by the out-of-phase mode described above, since the electron density is completely delocalized over both ring systems. These arguments suggest that the system may no longer behave as a pair of coupled oscillators, but rather as a single unit, leading to the possibility that only one mode for each totally symmetric vibration will be observed.

Surface Raman Spectra of the Viologen Monolayer on Au and Ag

As previously discussed (1,5), the thiol derivatives of viologens form self-assembled monolayers of high coverage on Au and Ag. This is shown by the cyclic voltammogram (CV) in Figure 6 (reproduced from the accompanying paper (1)). This CV clearly shows the two voltammetric waves for the viologen redox couple that were discussed in the accompanying paper (1), as well as the double peaked voltammetric signature that has been argued to be due to pi-merization. We now turn our attention to surface Raman spectroscopic measurements that unambiguously show this to be the case. The approach used is to obtain surface Raman spectra at -0.3 and -0.62 V where the pi-mer and monomer, respectively, are predominant, and then to compare these spectra with those of authentic monomer and pi-mer samples that were presented above.

The high molar absorptivities (ca. 10^4 M^{-1} cm^{-1} (45)) of both the pi-mer and the monomer in the visible absorption make it possible to detect surface (unenhanced) resonance Raman scattering of the cation radical on both gold and silver using appropriate excitation wavelengths. Figure 7 shows three sets of surface spectra, each set taken at two different potentials (-0.3 and -0.62 V), on silver and roughened silver electrodes. Several features of these spectra can be attributed to the presence of pi-mer within the SAM. In Figure 7A, one can clearly see that with 514 nm excitation, the relative intensity of the 1534 cm^{-1} band is large compared to the other bands at 1662, 1356, and 1028 cm^{-1}, while in Figure 7B, with 457 nm excitation, the 1534 cm^{-1} band is not relatively so enhanced. This is precisely the same behavior that

was observed in Figure 2 for the $(MV^{+\cdot})_2$ pi-mer, where excitation at 514 nm leads to large relative enhancement of the 1534 cm^{-1} band compared to excitation at 457 nm. We reiterate here that this behavior is consistent with expectations for resonant enhancement of the Raman spectrum of the pi-mer at 514 nm based on the electronic absorption spectrum for the dimer presented in Figure 1 above. Further, at both excitation wavelengths, the low energy band of the pi-mer is clearly observed at 1512 cm^{-1} as a shoulder on the 1534 cm^{-1} band (the shoulder at ca. 1640 cm^{-1} on the 1662 cm^{-1} band could be due to the HOH bending mode of water (47)). However this pi-mer band is not very clearly resolved in these spectra, a point to which we will return below. Finally, Figure 7C shows that the same trends of intensity versus excitation wavelength as well as the presence of the low energy pi-mer band are in evidence when the spectra are obtained on polished Ag versus roughened Ag electrodes. These experiments demonstrate that, at least qualitatively, the appearance of the pi-mer in these monolayers is not dependent on the gross morphology of the electrode surface.

The spectra in Figure 7 definitely demonstrate that the first, sharp shoulder on the first wave for these monolayers is due to the presence of the pi-mer in the monolayer. These same results have been reproduced many times for these viologen monolayers, and the connection between the first feature in the double-peaked CV wave and the spectroscopic signature of the pi-mer is unequivocal. However, while the relative intensities of the pi-mer features in

the voltammetry and the SERS spectra for a given monolayer were always roughly proportional, the amount of pi-mer formation was found to be a sensitive function of surface coverage, a point to which we return below. Further, given what the data in Figure 3 reveal about the relative Raman scattering cross-section for the monomer and pi-mer (with 457 nm excitation, the monomer cross-section is roughly the same as that of the pi-mer) the relative intensities of the low energy pi-mer bands in the SERS spectra seemed consistently below expectations based on the electrochemical data (i.e. the relative charges for the pi-mer and monomer peaks). To investigate the possible influence of the surface selection rule on this effect, we examined the surface (unenhanced) resonance Raman spectrum of these monolayers on a Au electrode.

Figure 8 shows three spectra in the 1470-1550 cm^{-1} region taken under conditions where there should be appreciable amounts of pi-mer present. Curve A is for a solution of 2 mM $MV^{+\cdot}$ (where [D]/[M] is ca. 0.4) with 457 nm excitation (i.e. off-resonance with respect to the pi-mer electronic transition at 536 nm). This spectrum shows the presence of a considerable amount of the pi-mer, based on the discussion presented above. Curve C shows a spectrum for a viologen monolayer on polished Ag, also with 457 nm excitation. In this case, even though the voltammetry suggested that the pi-mer comprised more than 30% of the monolayer, its presence is only barely revealed by a slight broadening on the low energy side of the band. Curve B shows a spectrum taken under similar conditions (with 488 nm excitation), but on a polished Au

electrode. In this case, the presence of the pi-mer is clearly indicated by the band at ca. 1508 cm^{-1}. Note that for both of the monolayers in curve B and C, the electrochemistry suggested the presence of large amounts of pi-mer.

An obvious question relates to the relatively large intensity of the pi-mer band on Au compared to silver surfaces. As alluded to above, we suggest that this effect is a consequence of the surface selection rule. In an earlier study (12), we showed that the orientation of the viologen group in these monolayers is such that the long axis of the viologen moiety is roughly perpendicular to the plane of the electrode. In this case, the surface selection rule for SERS on Ag using blue or green excitation would not favor observation of the q_i mode of the pi-mer, because the predominant polarizability change for this mode is normal to the planes of the viologen ring systems, and therefore roughly parallel to the metal surface. On the other hand, for blue or green excitation at a Au electrode, the surface selection rule is much less rigorous. This is because these excitation wavelengths are well above the plasmon resonance frequency of Au, leading to a much larger ratio of intensities of the parallel to perpendicular components of the exciting optical field. Under these conditions, there is little relative preference for modes with polarizability changes either parallel or perpendicular to the surface. Thus, the pi-mer q_i modes are easily observed, and have relative intensities that are roughly in accordance with expectations based on the electrochemical data.

Electrochemical consequences of pi-merization

There are many cases in the electrochemical literature in which unusually shaped cyclic voltammograms have been attributed to strong interactions between electroactive species that are confined at the electrode surface. At least three models have been presented that can be used to account for such interactions (8,9,48,49). Two of these (48,49) treat the interactions between adsorbates as manifesting themselves in the form of parameterized interfacial activity coefficients for the adsorbates that vary exponentially with surface coverage. In the present case, given that the interaction is due to a true chemical equilibrium between two monomeric V^+ radical cations to form a pi-mer, it might seem more appropriate to treat this as an E_rC_r case. This notation corresponds to a reversible electrochemical step followed by a reversible chemical step, which is essentially the treatment used for the case where the pi-mers form between solution phase species (25). However, a key difference between the solution case and the interfacial case is that, in solution, it is implicitly assumed that there are no constraints on the ability of the cation radicals to gain access to one another so as to acheive the equilibrium state. On the other hand, in the monolayer there may be many such constraints, an especially important one being an inability of the adsorbates to diffuse together. For the case of thiols or disulfides adsorbed at Au surfaces, while there are no direct measurements of the lateral diffusion coefficient, there is considerable evidence that surface diffusion is exceedingly slow

(50,51). This would imply that only that fraction of radical cations that are immediately adjacent to each other should be capable of forming pi-mers. It seems likely that this fraction would increase strongly with increasing surface coverage, since it is likely that electrostatic repulsion between adsorbates would cause them to be relatively well-distributed (i.e. as far apart as possible) at relatively low coverages, while the number of adjacent adsorbates would necessarily increase as the saturation coverage is approached. In fact, a lattice gas model (52) predicts that the number of nearest-neighbor contacts (i.e. between adjacent radical cations) should increase as the square of the viologen surface coverage.

To test the notion that the relative amount of pi-mer formation should depend on surface coverage, the ratio of monomeric radical cations to pi-mers was evaluated as a function of the surface coverage of viologen. In these experiments, the viologen SAM was formed from a relatively dilute solution (30 μM 1V12SH in 0.1 M NaCl) and a slightly elevated temperature (35 C), since these conditions were found to give more reproducible results. The experiments consisted of immersing a clean, vapor-deposited Au eletrode into a solution containing the viologen and periodically scanning the potential across the region of the first, one-electron reduction process (i.e. 0.0 to -0.65 V). The relative amounts of monomer and pi-mer were evaluated by integration of the voltammetric peaks after deconvolution (using fixed peak potentials determined from the values observed under conditions where the

monomer and pi-mer populations are similar, making the peak positions relatively easy to determine). The results are shown in Figure 9 as the fraction of reductive charge for pi-mer formation versus the total viologen surface coverage (i.e. monomer plus pi-mer). These data clearly show that pi-mer formation is a strong function of surface coverage. However, they do not appear to be qualitatively consistent with the expected squared dependence. They also show a very common feature of the pi-merization phenomenon, namely that we usually observe that only about 40-60% of the viologens in the monolayer can enter into the pi-mer, even at the highest attainable surface coverages. While it is possible to imagine causes for this (e.g. defectiveness of the monolayer induced by the microscopically rough Au surfaces), we have no experimental data that speak directly to its origin.

A final point concerns the difference in apparent formal potential for reduction into the monomeric and pi-meric states, which are -0.405 and -0.325 V, respectively (see Figure 6). Note that these values of the formal potential are not observed to be dependent on surface coverage, consistent with the two-state model described above (i.e. radical cations are either adjacent and capable of pi-merization or not). In such a case, the difference between the waves for reduction into the monomeric and pi-meric states (ΔE) should simply be given by $\Delta E = -\Delta G_{form}/2\mathcal{F}$ for the pi-merization process. Using this relation with the potentials given above gives a value of ΔG_{form} = -15.4 kJ mol^{-1}. There are several values of the formation constant for pi-merization of viologen

cation radicals (i.e. $K_{form} = 1/K_{diss}$) in the literature. These range from ca. 385 M^{-1} for dimethyl viologen cation radical (14) to 1100 M^{-1} for diethyl viologen cation radical (53), which give values for ΔG_{form} of -14.7 and -17.4 kJ mol^{-1}, respectively. That the experimental value is in very good agreement with previously reported values of ΔG_{form} supports the above discussion, and suggests that the presence of the viologen cation radicals in the monolayer does not appreciably alter their tendency toward pi-merization. It is worth noting that a calculation (54) of the extent of pi-merization expected within the monolayer using this range of K_{form} values predicts that pi-merization should be >99% complete, where this prediction is largely due to the very high local concentration of viologens at the interface.

Conclusions

The juxtaposition of adsorbates in SAM's can give rise to the manifestation of intermolecular interactions that are less frequently observed for isolated, monomeric species in solution. In the present case, congestion within the monolayer at high surface coverages leads to formation of dimerized π-complexes (pi-mers) between the one-electron reduced form of viologens in the SAM's, as shown by the surface Raman data. This pi-merization leads to structure (i.e. multiple peaks) in the voltammetry of the SAM. Thus, this study has provided a direct correlation between the non-ideal (macroscopic) voltammetric behavior of a surface confined redox species and its (microscopic) molecular behavior. The lower energy Raman bands in the fundamental ring mode region

(below 1700 cm^{-1}) that are due exclusively to the pi-mer have also been assigned to the q_i modes that arise from out-of-phase coupling of the totally symmetric ring modes of the component cation radicals in the pi-mer.

The data presented here indicate that a relatively wide range of behavior is observed with respect to the extent of viologen cation radical pi-mer formation under different conditions. For example, for MV^+, relatively high solution concentrations are required to effect pi-mer formation. On the other hand. for the n=3 system, pi-merization in aqueous solutions is virtually complete under all conditions. Intermediate behavior is observed for the $1V^+12$ species which is capable of micellization. As mentioned above, the viologen monolayers studied here exhibited only an intermediate extent of dimer formation, even at the highest attainable surface coverages. However, the two state model presented above suggests that this is due not to monomer/pi-mer equilibria between adjacent radicals, but rather is controlled by the fraction of radicals that have neighbors close enough to allow pi-merization. In other words, when a neighbor exists, pi-merization occurs (essentially to completion); when no neighbor exists only monomeric radicals are produced.

A important conclusion of this study is that the high local concentrations of species within interfacial assemblies can lead to behavior that is predominantly representative of the types of interactions that can occur between adsorbates. This observation is no doubt largely due to the high local concentration of species in

such assemblies.

Acknowledgements

We gratefully acknowledge the Office of Naval Research for the full support of this work, and James Walker for providing the data in Figure 9.

REFERENCES

1. Schneider, T.S.; Buttry, D.A. Langmuir **1994**, 10, 0000-0000.

2. Murray, R. W. in Electroanalytical chemistry; Bard, A. J., Ed; Marcel Dekker: New York, 1983, p.191.

3. Lee, C.-W.; Bard, A. J. J. Electroanal. Chem. **1988**, 239, 441-446.

4. Lee, C.-W.; Bard, A. J. Chem. Phys. Lett. **1990**, 170, 57-60.

5. De Long, H. C.; Buttry, D. A. Langmuir **1990**, 6, 1319-1322.

6. Schneider, T., Ph.D. Thesis, University of Wyoming, 1993.

7. Park, S. G.; Aoki, K.; Tokuda, K.; Matsuda, H. J. Electroanal. Chem. **1985**, 195, 157-163.

8. Matsuda, H.; Aoki, K.; Tokuda, K. J. Electroanal. Chem. **1987**, 217, 1-13.

9. Matsuda, H.; Aoki, K.; Tokuda, K. J. Electroanal. Chem. **1987**, 217, 15-32.

10. Bruinink, J.; Kregting, C. G. A.; Ponjee, J. J. J. Electrochem. Soc. **1977**, 124, 1854-1858.

11. Gomez, M.; Li, J.; Kaifer, A. G. Langmuir, **1991**, 7, 1797-1806.

12. Tang, X.; Schneider, T.; Buttry, D. A., submitted to Langmuir.

13. Poizat, O.; Sourisseau, C.; Corset, J. J. Mol. Struc. **1986**, 143, 203-206.

14. Schwarz Jr., E. M., Ph.D. Thesis, University of Wisconsin 1961.

15. Kosower, E. M.; Cotter, J. L. J. Am. Chem. Soc. **1964**, 86, 5524-5527.

16. Evans, A. G.; Evans, J. C.; Baker, M. W. J. Chem. Soc., Perkin II **1977**, 1787-1789.

17. Evans, A. G.; Evans, J. C.; Baker, M. W. J. Chem. Soc., Perkin II, **1975**, 1310-1311.

18. Itoh, M.; Kosower, E. M. J. Am. Chem. Soc. **1968**, 90, 1843-1849.

19. Itoh, M. J. Am. Chem. Soc. **1971**, 93, 4750-4754.

20. Itoh, M. J. Am. Chem. Soc., **1972**, 94, 1034-1035.

21. Furue, M.; Nozakura, S. Chem. Lett. **1980**, 821-824.

22. Furue, M.; Yamanaka, S.; Phat, L.; Nozakura, S. J. Polym. Sci. **1981**, 19, 2635-2646.

23. Furue, F.; Nozakura, S. Bull. Chem. Soc. Jpn. **1982**, 55, 513-516.

24. Imabayashi, S.; Kitamura, N.; Tokuda, K. Chem. Lett. **1987**, 915-918.

25. Imabayashi, S.; Kitamura , N.; Tokuda, K. J. Electroanal. Chem. **1988**, 243, 143-160.

26. Lu, T.; Cotton, T. M.; Hurst, J. K.; Thompson, D. H. P. J. Phys. Chem. **1988**, 92, 6978-6985.

27. Hausser, K. H.; Murrell, J. N. J. Chem. Phys. **1957**, 27, 500-504.

28. Kosower, E. M.; Hajdu, J. J. Am. Chem. Soc. **1971**, 93, 2534-2535.

29. Kosower, E. M. In "Free Radicals in Biology", Vol. II; Pryor, W. A., Ed; Academic Press: New York, 1976, Chapter 1.

30. Forster, M.; Girling, R. B.; Hester, R. E. J. Raman Spec. **1982**, 12, 36-48.

31. Hester, R. E.; Suzuki, S. J. Phys. Chem. **1982**, 86, 4626-4630.

32. Ghoshal, S.; Lu, T.; Feng, Q.; Cotton, T. M. Spectrochim. Acta **1988**, 44A, 651-660.

33. Ito, M.; Sasaki, H.; Takahashi, M. J. Phys. Chem. **1987**, 91, 3932-3934.

34. Sasaki, H.; Takahashi, M.; Ito, M. J. Electron Spec. Rel. Phen. **1987**, 45, 161-168.

35. Christensen, P. A.; Hamnett, A. J. Electroanal. Chem. **1989**, 49-68.

36. Bae, I. T.; Huang, H.; Yeager, E. B.; Scherson, D. A. Langmuir, **1991**, 7, 1558-1562.

37. Mulliken, R. S., Person, W. B. "Molecular Complexes"; Wiley-Interscience: New York, 1969, Chap. 5.

38. Ferguson, E. E.; Matson, F. A. J. Chem. Phys. **1958**, 29, 105-

107.

39. (a) Bozio, R.; Feis, A.; Pecile, C. J. Chem. Phys. **1989**, 91, 13-19. (b) Meneghetti, M.; Bozio, R.; Zanon, I.; Pecile, C.; Ricotta, C.; Zanetti, M. J. Chem. Phys. **1984**, 80, 6210-6224. (c) Girlando, A.; Marzola, F.; Pecile, C.; Torrance, J. B. J. Chem. Phys. **1983**, 79, 1075-1085. (d) Girlando, A.; Bozio, R.; Pecile, C.; Torrance, J. B. Phys. Rev. B **1982**, 26, 2306-2309. (e) Bozio, R.; Pecile, C. In "The Physics and Chemistry of Low Dimensional Solids"; Alcacer, L. Ed; D. Reidel:New York; 1980, p.165-186. (f) Bozio, R.; Zanon, I.; Girlando, A.; Pecile, C. J. Chem. Phys. **1979**, 71, 2282-2293. (g) Bozio, R.; Girlando, A.; Pecile, C. Chem. Phys. **1977**, 21, 257-263.

40. (a) Rice, M. J.; Yartsev, V. M.; Jacobson, C. S. Phys. Rev. B **1980**, 21, 3437-3446. (b) Rice, M. J.; Nordita A. Solid State Comm. **1979**, 31, 93-98. (c) Lipari, N. O.; Rice, M. J.; Duke, C. B.; Bozio, R.; Girlando, A.; Pecile, C. Intl. J. Quant. Chem., Quant. Chem. Symp. **1977**, 11, 583-594. (d) Rice, M. J.; Lipari, N. O.; Strassler, S. Phys. Rev. Lett. **1977**, 39, 1359-1362.

41. Yarwood, J. "Spectroscopy and Structure of Molecular Complexes"; Plenum Press: New York, 1973.

42. "Advances in Infrared and Raman Spectroscopy"; Vol.4; Clark, R. J. H., Hester, R. E., Eds; Heyden: London, 1978, Chap. 1.

43. (a) Hinkel, J. J.; Devlin, J. P. J. Chem. Phys. **1973**, 58, 4750-4756. (b) Anderson, G. R.; Devlin, J. P. J. Phys. Chem. **1975**, 79, 1100-1102.

44. (a) Tang, J.; Albrecht, A. C. In "Raman Spectroscopy Theory and Practice"; Szymanski, H. A., Ed; Plenum: New York-London, 1970, Chap. 2. (b) Johnson, B. B.; Peticolas, W. L. Ann. Rev. Phys. Chem. **1976**, 27, 465-491. (c) Spiro, T. G.; Stein, P. Ann. Rev. Phys. Chem. **1977**, 28, 501-521.

45. Stargardt, J.; Hawkridge, F. M. Anal. Chim. Acta **1983**, 146, 1-8.

46. Doorn, S. K.; Blackbourn, R. L.; Johnson, C. S.; Hupp, J. T. Electrochim. Acta **1991**, 36, 1775-1785.

47. Osawa, M.; Suetaka, W. J. Electroanal. Chem. **1991**, 270, 261-272.

48. Laviron, E. J. Electroanal. Chem. **1974**, 52, 395-402.

49. Brown, A.P.; Anson, F.C. Anal. Chem. **1977**, 49, 1589-95.

50. Folkers, J.P.; Laibinis, P.E.; Whitesides, G.M.; Deutch, J.

Langmuir **1994**, 98, 563-71.

51. Ross, C.B.; Sun, L.; Crooks, R.M. Langmuir, **1993**, 9, 632-36.

52. Lane, J.E. In "Adsorption from Solution at the Solid/Liquid Interface"; Parfitt, G.D., Rochester, C.H., Eds.; Academic Press: New York, 1983; Chapter 2, p. 69.

53. Evans, A.G.; Evans, J.C.; Baker, M.W. J. Am. Chem. Soc. **1977**, 99, 5882-84.

54. The calculation is done using the given values of K_{form} and effective volume concentrations of the viologen species in the monolayer, where these are calculated from the surface coverages for each species, Γ_i, and the effective thickness, d, of the monolayer (taken to be ca. 20 Å) using the relation $\Gamma_i/d = C_i$, where C_i is the concentration.

Table 1

1. Resonant Raman Bands of $(MV^{+})_2$ and MV^{+}.*

$(MV^{+\cdot})_2$	q_i	1028	1340	1512	1604
	s_i	1028	1356	1534	1662
$MV^{+\cdot}$	Q_i	1028	1456	1534	1662

* Data from reference 30.

Figure Captions

1. Absorption spectra of (A) 1 mM $1V^+3V^+1$; (B) 0.3 mM $2V^+12$; (C) 0.3 mM $MV^{\cdot}$ in water formed by dithionite reduction.

2. Resonant Raman spectra of 5 mM MV^+ formed by dithionite reduction at two different excitation wavelengths: (A) 514 nm; (B) 457 nm. All relative intensities are normalized to the intensity of the 1534 cm^{-1} band.

3. Resonant Raman spectra of 1, 2 and 5 mM MV^+ formed by dithionite reduction using (A) 457 nm and (B) 514 nm excitations.

4. Resonant Raman spectra at 514, 488 and 457 nm excitations of ca. 0.3 mM $2V^+12$.

5. Resonant Raman spectra at 514, 488, and 457 nm excitation of $1V^+3V^+1$ (less than 3 mM).

6. Voltammogram of 1V12SH at saturation coverage (Γ = 3.1 x 10^{-10} mol cm^{-2}) on smooth Au in 0.1 M $NaNO_3$ with a scan rate of 100 mV/s, referenced versus SSCE.

7. SERRS spectra of (A) 1V16SH, with 514 nm excitation and (B) 1V12SH, with 457 nm excitation on roughened silver electrode in 0.1 M $NaNO_3$; (C) surface Raman resonant spectra of 1V12SH on polished silver electrode in 0.1 M $NaNO_3$ with 457 nm excitation, referenced versus Ag/AgCl.

8. Resonant Raman spectrum of (A) 2 mM MV^+, 457 nm excitation; (B) 1V12SH on gold electrode at -0.62 V vs Ag/AgCl in 0.1 M NaCl, 488 nm excitation and (C) 1V12SH on polished silver electrode at -0.62 V vs Ag/AgCl in 0.1 M $NaNO_3$, excitation 457 nm.

9. Plot of fraction of viologen in pi-mer (Γ_D/Γ_{D+M}) versus fractional surface coverage, where Γ_D = dimer surface coverage, Γ_{D+M} = dimer plus monomer surface coverage, and Γ_T = total surface coverage at saturation (i.e. at highest attainable coverage).

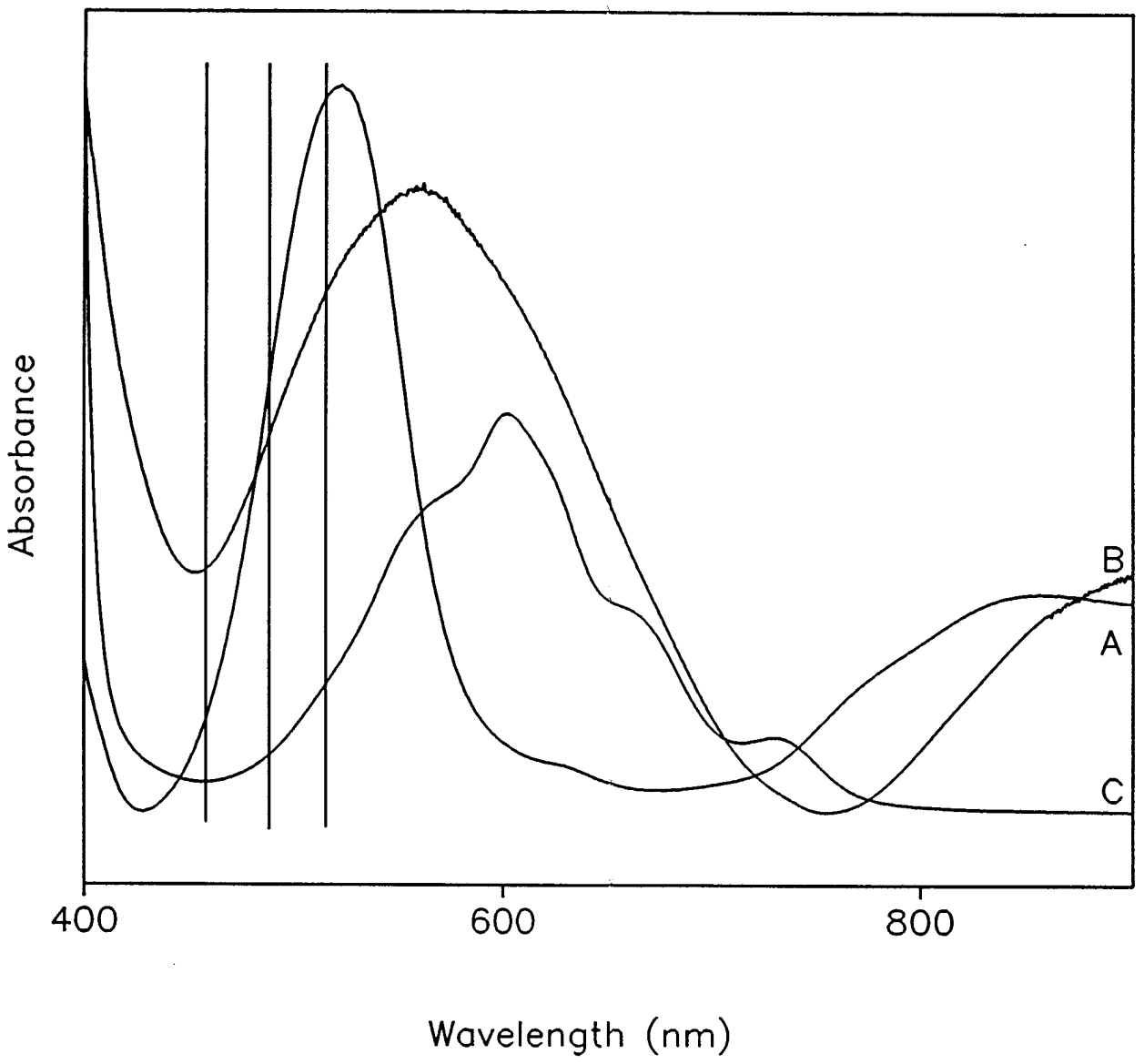
Absorbance
400
600
800
Wavelength (nm)
B
A
C

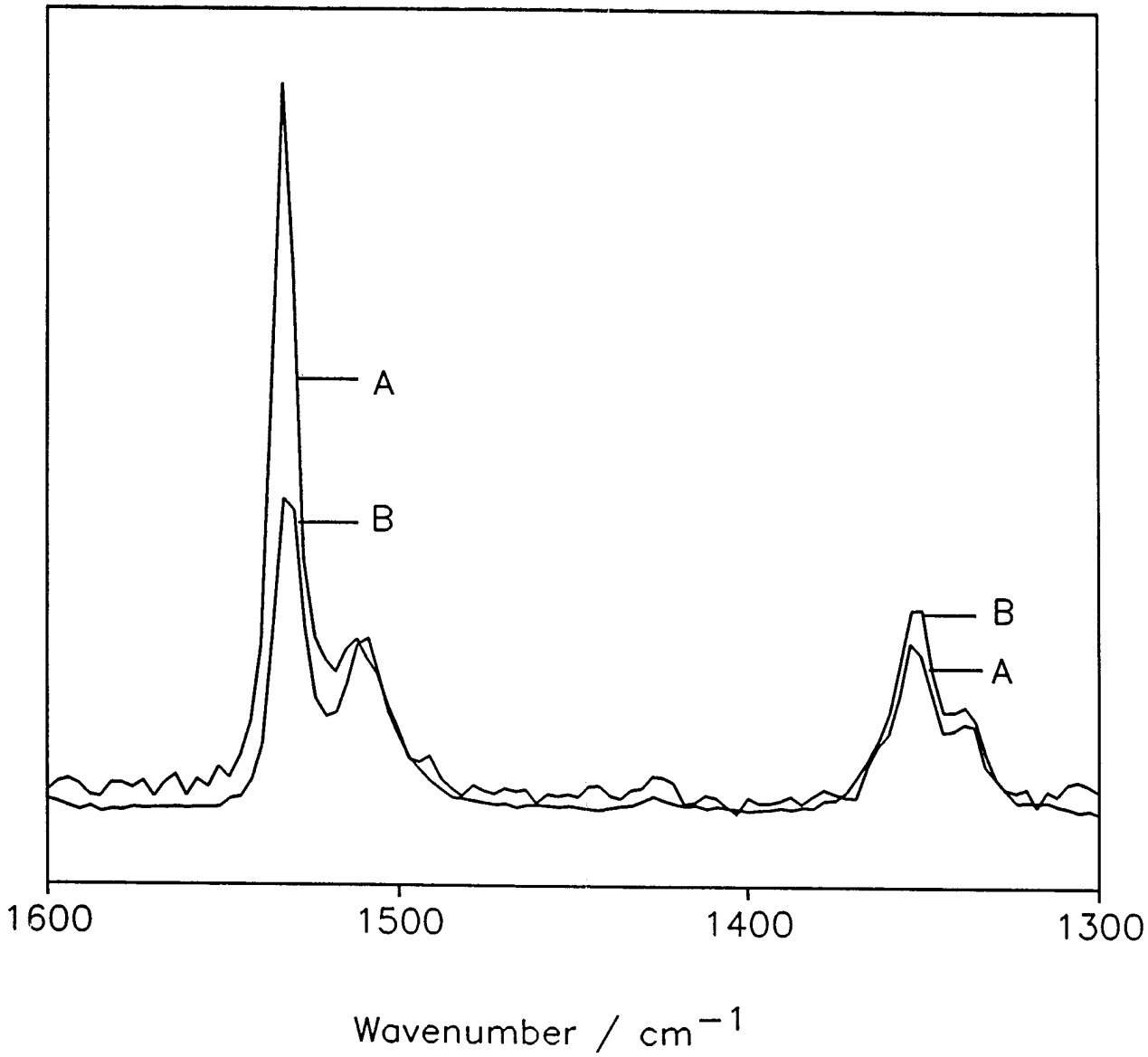
A
B
B
A
1600
1500
1400
1300
Wavenumber / cm^{-1}

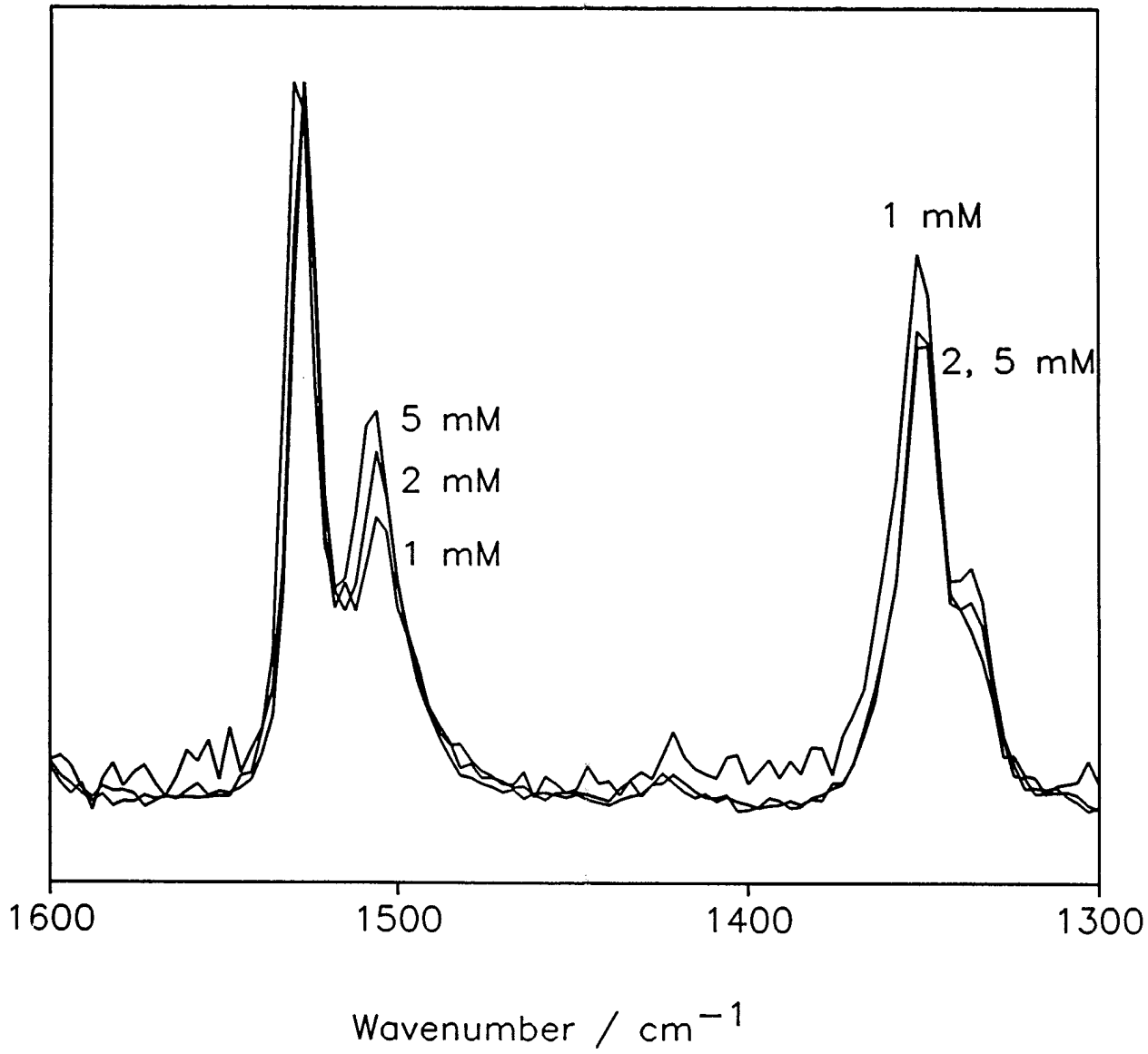
1 mM
2, 5 mM
5 mM
2 mM
1 mM
1600
1500
1400
1300
Wavenumber / cm^{-1}

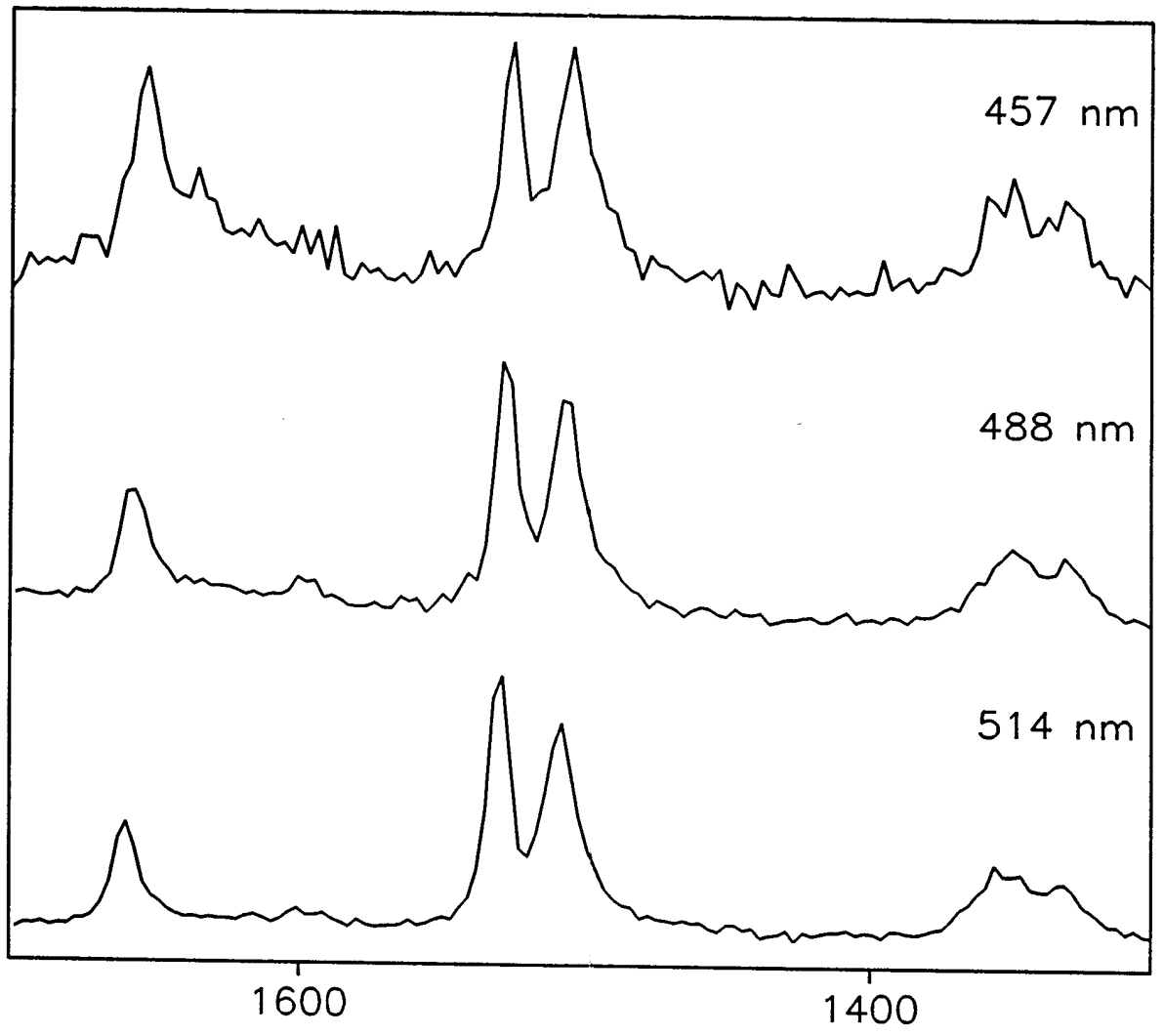
457 nm
488 nm
514 nm
1600
1400
Wavenumber / cm^{-1}

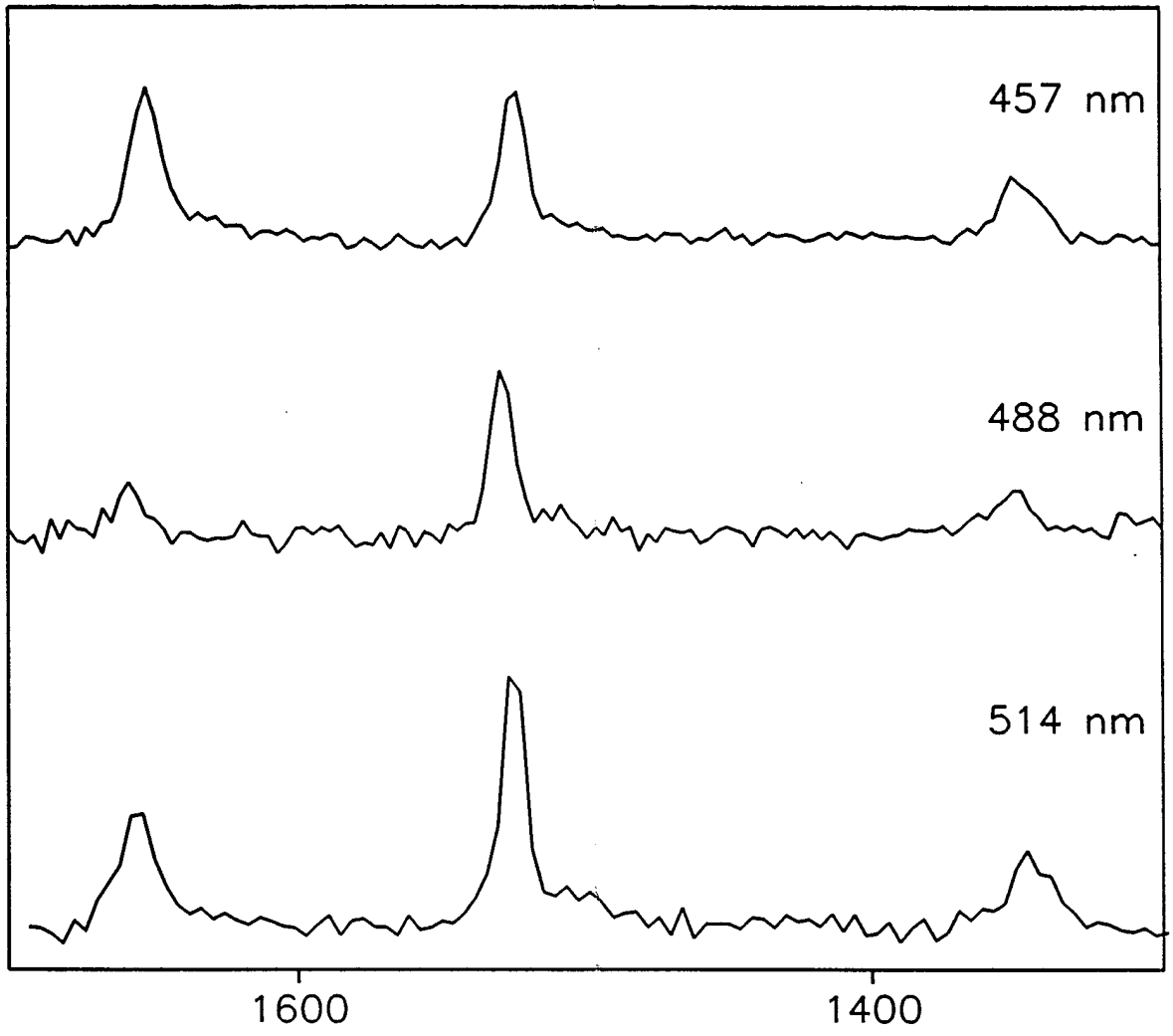
457 nm
488 nm
514 nm
1600
1400
Wavenumber / cm^{-1}

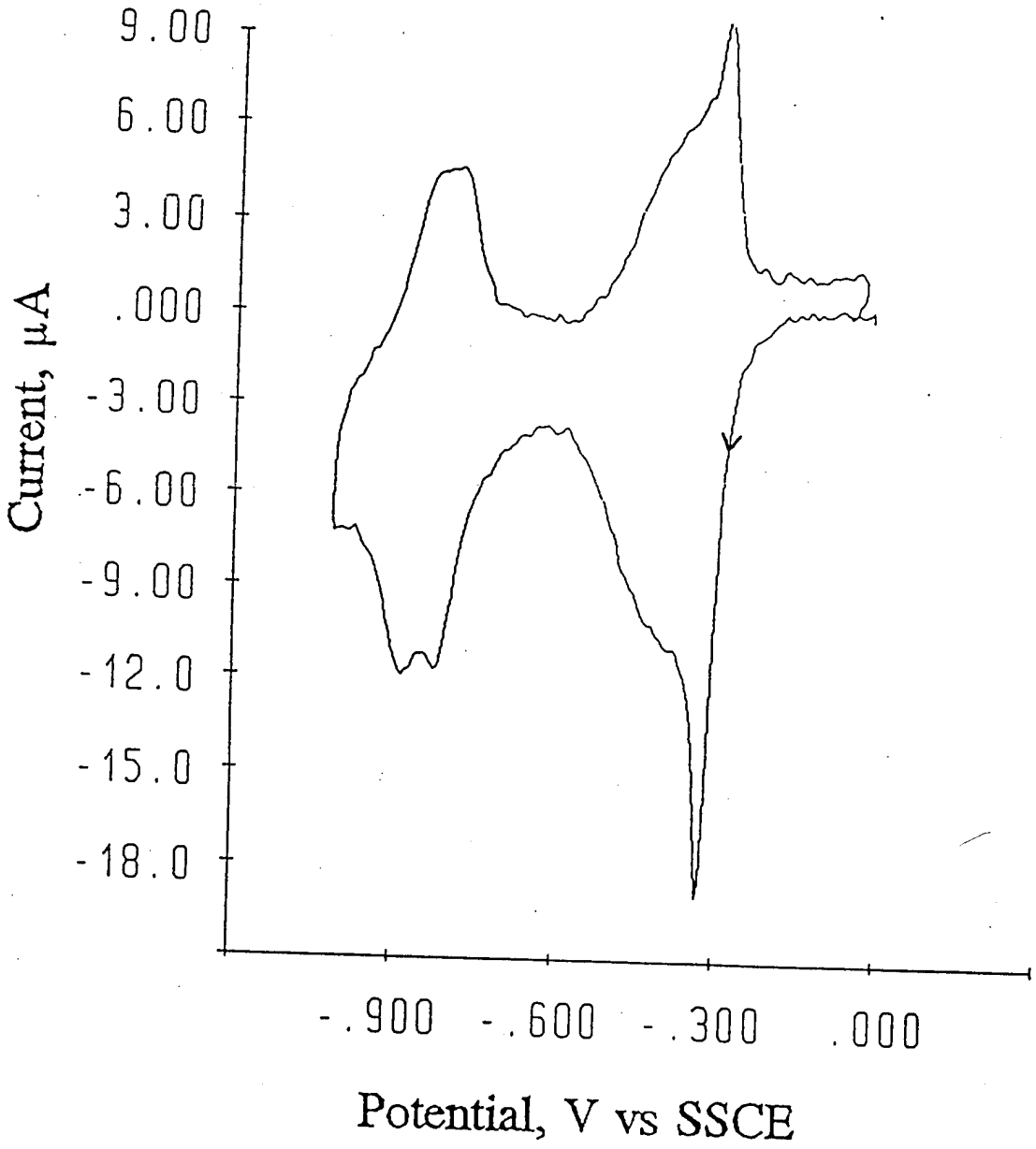
9.00
6.00
3.00
.000
-3.00
-6.00
-9.00
-12.0
-15.0
-18.0
Current, µA
-.900
-.600
-.300
.000
Potential, V vs SSCE

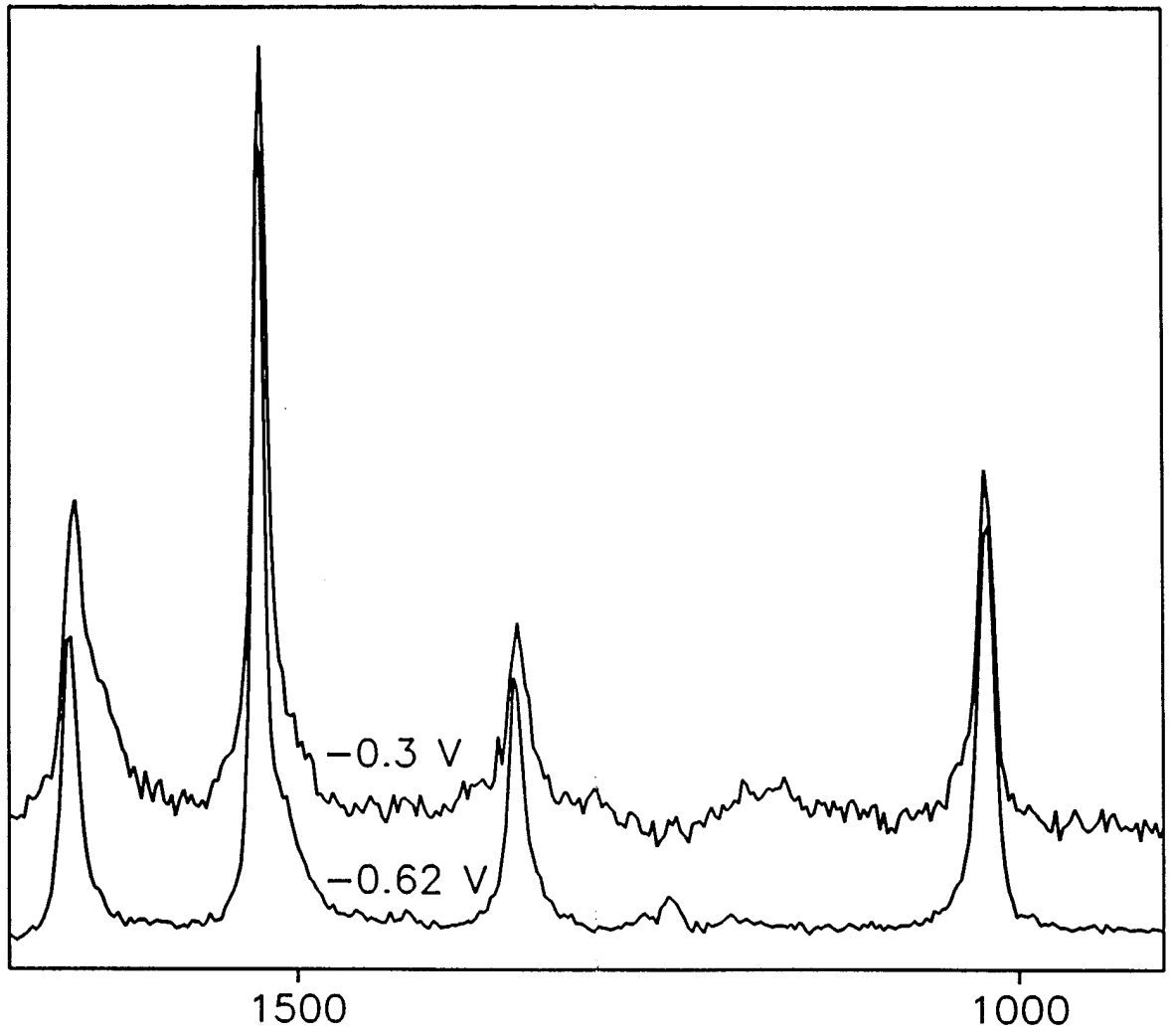
−0.3 V
−0.62 V
1500
1000
Wavenumber / cm^{-1}

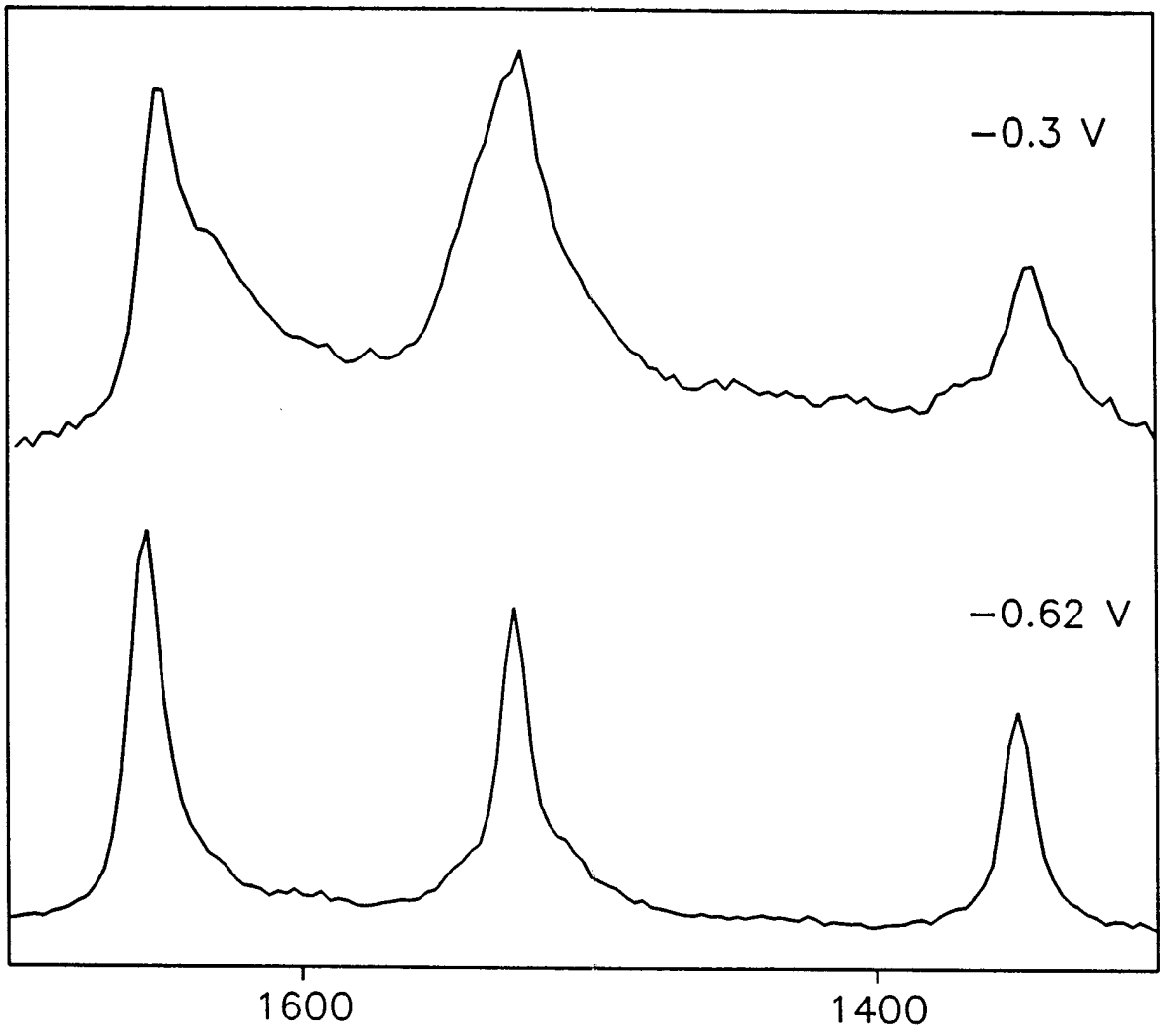
−0.3 V
−0.62 V
1600
1400
Wavenumber / cm^{-1}

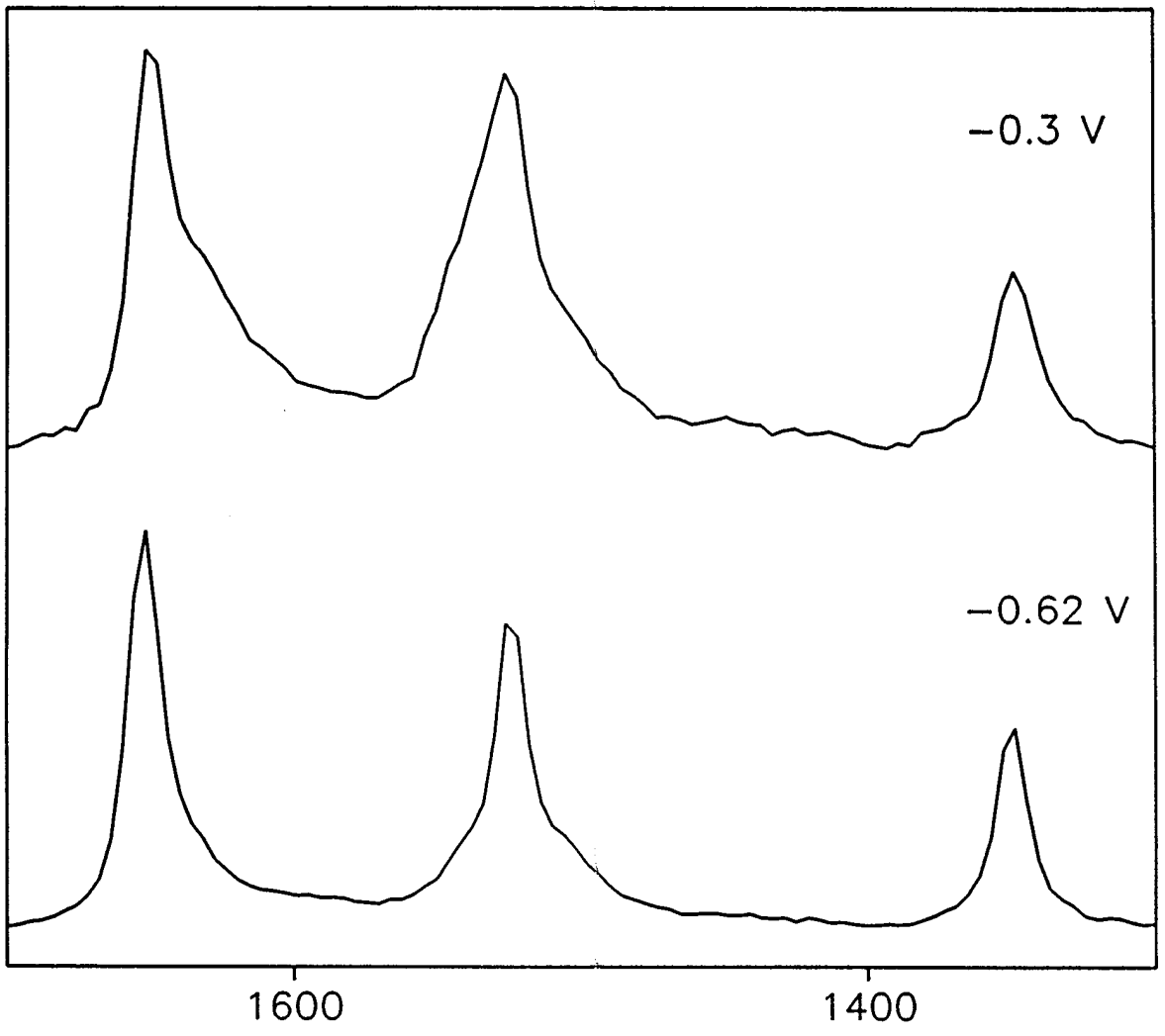
−0.3 V
−0.62 V
1600
1400
Wavenumber / cm^{-1}

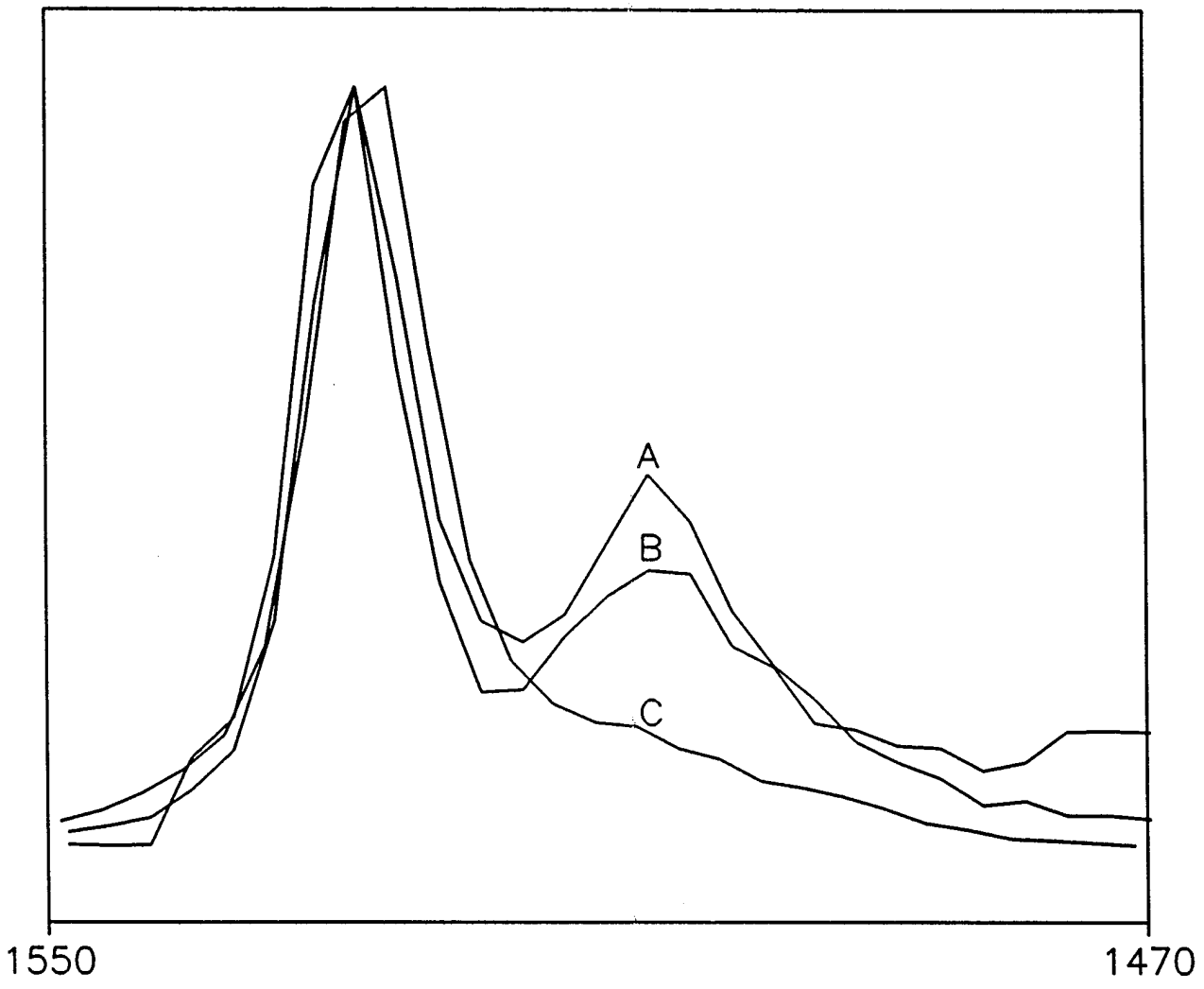
A
B
C
1550
1470
Wavenumber / cm^{-1}

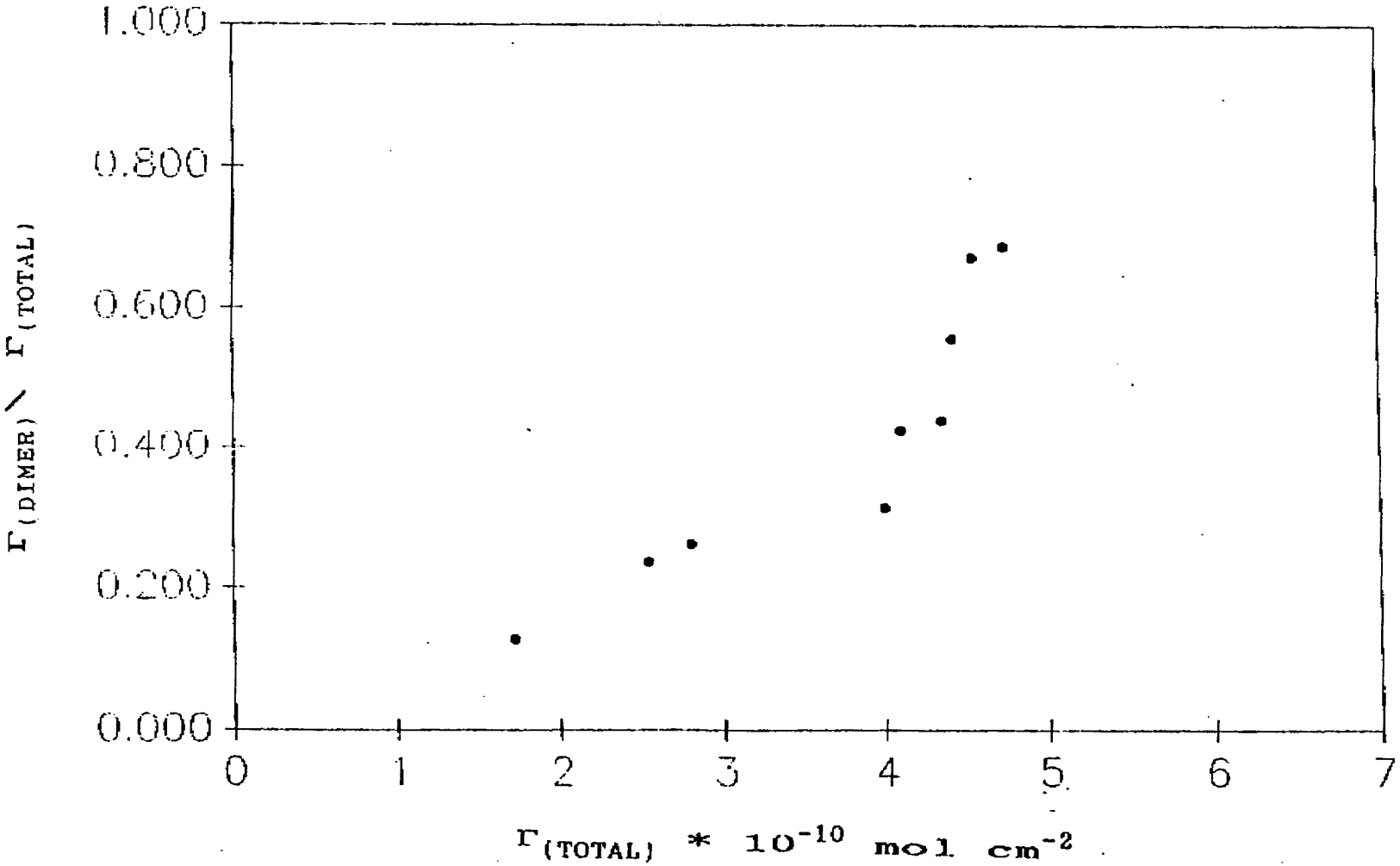
1.000
0.800
0.600
0.400
0.200
0.000
0
1
2
3
4
5
6
7
Γ(DIMER) \ Γ(TOTAL)
Γ(TOTAL) * 10-10 mol cm-2